Progress In Electromagnetics Research Letters, Vol. 30, 1–12, 2012

CHARACTERIZATION OF TWO-DIMENSIONAL LEFT-HANDED TRAVELING-WAVE FIELD-EFFECT TRANSISTORS

K. Narahara*

Graduate School of Science and Engineering, Yamagata University, 4-3-16 Jonan, Yonezawa, Yamagata 992-8510, Japan

Abstract—The characteristics of a two-dimensional (2D) left-handed traveling-wave field-effect transistor, which is two 2D composite rightand left-handed (CRLH) transmission lines with both passive and active couplings, are discussed for generating non-attenuated waves having left-handedness in 2D. In this study, the design criteria for wave amplification are described, and the results from numerical calculations obtained by solving the transmission equations for the device are presented.

1. INTRODUCTION

Composite right- and left-handed (CRLH) transmission lines have been extensively studied, and several important breakthroughs have been achieved in the management of electromagnetic continuous waves [1] both in one (1D) and two dimensions (2D). CRLH lines have a single series and shunt inductance-capacitance (LC) pair in each unit cell. They exhibit left-handedness, i.e., at certain frequencies, their phase velocity has a sign opposite to that of their group velocity. In addition, the 2D CRLH lines exhibit extraordinary refractive properties [2–6]. Figure 1 shows the unit cell of a 2D CRLH line, where L_R, C_L, L_L, and C_R are the series inductance, series capacitance, shunt inductance, and shunt capacitance, respectively. The series LC pair consists of L_R and C_L, and the shunt pair consists of L_L and C_R. These parameters define the upper and lower zero-wavelength frequencies of the CRLH line, which are given by $\omega_u = \max(1/\sqrt{C_L L_R}, 1/\sqrt{C_R L_L})$ and $\omega_l = \min(1/\sqrt{C_L L_R}, 1/\sqrt{C_R L_L})$, respectively. The line exhibits right-handedness at frequencies greater than ω_u and left-handedness

Received 29 November 2011, Accepted 29 December 2011, Scheduled 8 February 2012
* Corresponding author: Koichi Narahara (narahara@yz.yamagata-u.ac.jp).

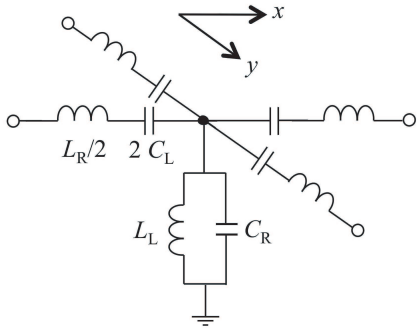

Figure 1. Unit cell of a 2D CRLH line.

at frequencies lower than ω_l. A frequency band gap exists between ω_l and ω_u in which all supporting modes are evanescent.

The use of CRLH lines may sometimes be impractical because of their finite electrode resistance and substrate current leakage, and may require loss compensation schemes. Recently, several authors have investigated methods for amplifying LH waves in 1D using transistors [7–9]. In particular, we analyze the use of two CRLH lines that interact continuously via transistor transconductance together with both capacitive and inductive couplings and successfully obtain the design criteria for wave amplification in such a device. In this study, we extend the method into a 2D platform, i.e., we investigate the two 2D CRLH lines coupled both passively and actively, which we call a 2D CRLH traveling-wave field-effect transistor (TWFET), or 2D CRLH TWFET for brevity. In addition, we discuss the design criteria for wave amplification in 2D CRLH TWFETs, together with several fundamental properties including the device configuration, dispersion relationship, and characteristic impedance. We show that the design criteria for a 1D line are valid with no alteration required for long-wavelength waves. Next, we discuss the results of numerical calculations, which confirm the validity of the criteria and demonstrate the wave refraction at the interface between the LH and RH regions.

2. 2D CRLH TWFETS

Figure 2 shows unit-cell structure of a 2D CRLH TWFET. It is best to use multilevel substrate technology and sufficient to use simple bonding wire. Inclusion of a chip inductor can improve design flexibility. The lines TL_G and TL_D, which are periodically connected to the gate and drain of an FET, represent the gate and drain lines, respectively. Each

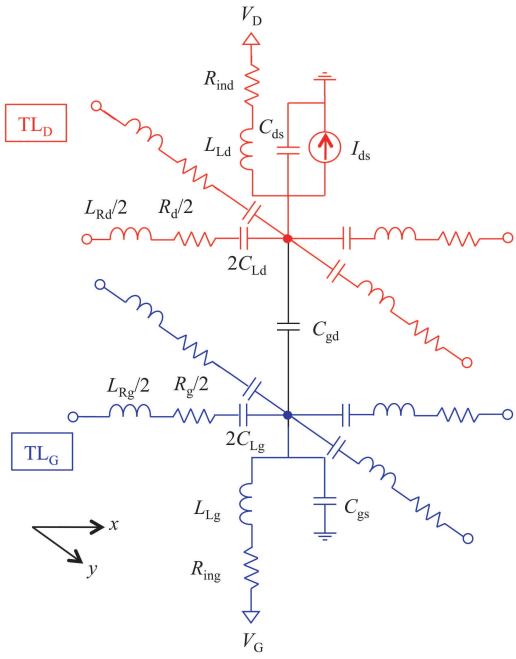

Figure 2. Unit-cell structure of a 2D CRLH TWFET. Red and blue symbols represent the drain and gate lines, respectively.

section of line $TL_{G,D}$ is connected to the electrode that is biased at $V_{G,D}$. It is expected that waves on the lines experience amplification by the transconductance effect between TL_D and TL_G. L_{Rg}, C_{gs}, L_{Lg}, and C_{Lg} are the RH inductance, RH capacitance, LH inductance, and LH capacitance of the gate CRLH line, respectively. C_{gd} and I_{ds} are the mutual capacitance and drain-source current, respectively. R_g, R_d, R_{ing}, and R_{ind} are the gate series resistance, drain series resistance, gate shunt conductance, and drain shunt conductance, respectively. The gate and drain of each FET can be biased by V_G and V_D via L_{Lg} and L_{Ld}, respectively. Because of the skin effect and dielectric relaxation, electrode losses are generally frequency dispersive. However, we characterize the losses by simple non-dispersive resistors; therefore, our model can be applied only to narrow-band applications.

First, we characterize the 2D CRLH TWFETs whose loaded FETs are all pinched off. Owing to the presence of the passive coupling between the gate and drain lines, two different propagation modes can carry the waves on 2D CRLH TWFETs. See Gupta et al. [10]

for comprehensive description of the modes in coupled lines. Each mode has its own characteristic impedance, dispersion, and the voltage fraction between the lines. Mostly, there are four zero-wavelength frequencies given by

$$\omega_{0a} = \frac{1}{\sqrt{C_{Lg}L_{Rg}}}, \tag{1}$$

$$\omega_{0b} = \frac{1}{\sqrt{C_{Ld}L_{Rd}}}, \tag{2}$$

$$\omega_{0c} = \frac{\sqrt{2}}{\sqrt{X + \sqrt{(C_{ds}L_{Ld} - C_{gs}L_{Lg})^2 + Y}}}, \tag{3}$$

$$\omega_{0d} = \frac{\sqrt{2}}{\sqrt{X - \sqrt{(C_{ds}L_{Ld} - C_{gs}L_{Lg})^2 + Y}}}, \tag{4}$$

where

$$X = C_{ds}L_{Ld} + C_{gs}L_{Lg} + C_{gd}(L_{Ld} + L_{Lg}), \tag{5}$$

$$Y = C_{gd}[C_{gd}(L_{Ld} + L_{Lg})^2 + 2(L_{Ld} - L_{Lg}) \times (C_{ds}L_{Ld} - C_{gs}L_{Lg})]. \tag{6}$$

For zero mutual capacitance, the resonant frequencies corresponding to the series and shunt LC pairs in the gate and drain lines define the zero-wavelength frequencies, which we call $\omega_{seg} \equiv 1/\sqrt{C_{Lg}L_{Rg}}$, $\omega_{sed} \equiv 1/\sqrt{C_{Ld}L_{Rd}}$, $\omega_{shg} \equiv 1/\sqrt{C_{gs}L_{Lg}}$ and $\omega_{shd} \equiv 1/\sqrt{C_{ds}L_{Ld}}$. Because the mutual inductance is ignored, ω_{0a} and ω_{0b} coincide with ω_{seg} and ω_{sed}, respectively. The other two frequencies ω_{0c} and ω_{0d} are defined by the shunt LC pairs and are influenced by the mutual capacitance, i.e., ω_{0c} and ω_{0d} correspond to $\min(\omega_{shg}, \omega_{shd})$ and $\max(\omega_{shg}, \omega_{shd})$, respectively. Both ω_{0c} and ω_{0d} decrease because of the finite mutual capacitance.

The dispersion originally depends on the x and y components of the 2D wave vector in a different manner. However, the line becomes isotropic for long wavelengths, such that the dispersion only depends on the amplitude of the wave vector. We first assume that the long wavelength approximation is valid.

Figure 3 shows a sample dispersion relationship for the line parameters listed in Table 1. The reactances in Table 1 were designed for the fast and slow mode branches to have a cross point corresponding to the frequency at which the long wavelength approximation could be properly applied for C_{gd}=0. In addition, the value of C_{gd} was designed for the gate and drain lines to exhibit moderate voltage fractions. The

Table 1. Sample line parameters.

L_{Rg}(nH)	0.75	L_{Rd}(nH)	1.0
C_{Lg}(pF)	1.5	C_{Ld}(pF)	2.0
L_{Lg}(nH)	1.25	L_{Ld}(nH)	0.5
C_{gs}(pF)	1.0	C_{ds}(pF)	1.5
C_{gd}(pF)	0.2		

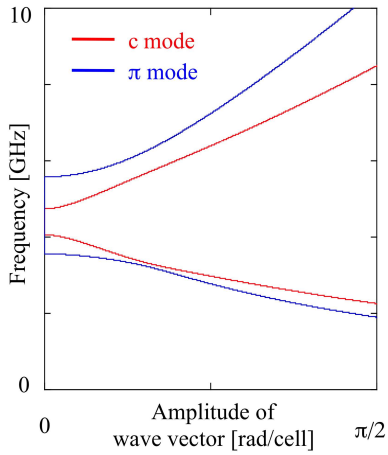

Figure 3. Dispersion relationship of 2D CRLH TWFETs for parameters listed in Table 1.

upper two frequencies are degenerated. Hereafter, we call the fast and slow modes for a given frequency the π- and c-modes, respectively; therefore, the red and blue curves in Figure 3 correspond to the c- and π-modes, respectively. The zero-wavelength frequencies f_{cl}, f_{cu}, $f_{\pi l}$, and $f_{\pi u}$ are 4.1, 4.7, 3.6, and 5.6 GHz, respectively.

Let the amplitude of the wave vector of the $c(\pi)$-mode be denoted as $k_{c(\pi)}(\omega)$ for an angular frequency ω. It follows that the characteristic impedances of the $c(\pi)$-mode are given by

$$Z_{c(\pi),g}(\omega) = \frac{-1 + L_{Rg}C_{Lg}\omega^2}{C_{Lg}\omega k_{c(\pi)}(\omega)}, \tag{7}$$

$$Z_{c(\pi),d}(\omega) = \frac{-1 + L_{Rd}C_{Ld}\omega^2}{C_{Ld}\omega k_{c(\pi)}(\omega)}, \tag{8}$$

where $Z_{c(\pi),g}$ and $Z_{c(\pi),d}$ are with respect to the gate and drain

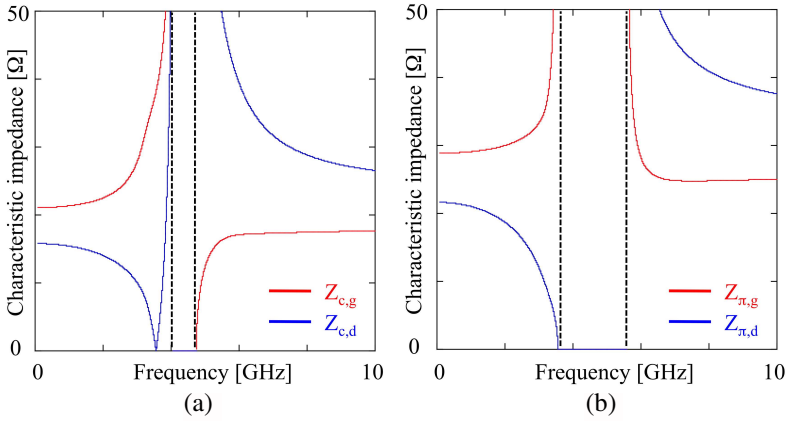

Figure 4. Characteristic impedances of 2D CRLH TWFETs for parameters listed in Table 1. (a) The c-mode and (b) π-mode impedances. Red and blue curves represent the gate and drain lines, respectively. Dashed lines represent the cut-off frequencies.

lines, respectively. Figures 4(a) and (b) show the c- and π-mode characteristic impedances, respectively, for the line parameters listed in Table 1. Near the cut-off frequencies, the characteristic impedances significantly depend on the frequency, and approach infinity or zero at the cut-off frequencies. For waves propagating in the $\mathbf{k} = (k_x, k_y)$ direction, the matched impedances in the x and y directions are given by $k_x Z/|\mathbf{k}|$ and $k_y Z/|\mathbf{k}|$, respectively, where Z denotes the characteristic impedance.

In addition, the voltage fractions between the gate and drain lines are given by

$$R_{c(\pi)} = \frac{-k_{c(\pi)}(\omega)\omega - Z_{c(\pi),g}(1 - (C_{gd} + C_{gs})L_{Lg}\omega^2)}{C_{gd}L_{Lg}Z_{c(\pi),g}(\omega)\omega^2}. \tag{9}$$

The voltage fractions are shown in Figure 5 for the parameters listed in Table 1. In the figure, the red and blue curves represent these fractions for the c- and π-modes, respectively. When the voltage fraction is positive (negative), the corresponding mode becomes in phase (out of phase). Therefore, the π-mode becomes out of phase and in phase at the LH and RH frequencies, respectively. On the other hand, the c-mode becomes out of phase for the RH frequencies. In addition, R_c becomes zero at some LH frequency, where $Z_{c,g}$ vanishes. At that frequency, the c-mode reverses its parity.

By introducing a small transconductance G_m, we can obtain the

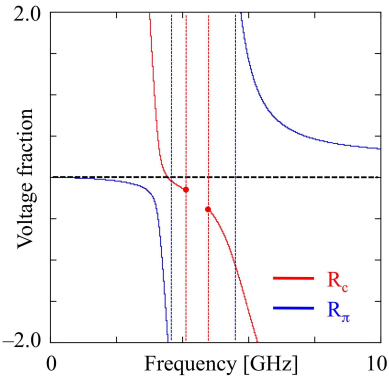

Figure 5. Voltage fraction between lines for 2D CRLH TWFETs for parameters listed in Table 1. Dashed lines represent the cut-off frequencies. Red and blue curves and lines represent that of the c- and π-modes, respectively.

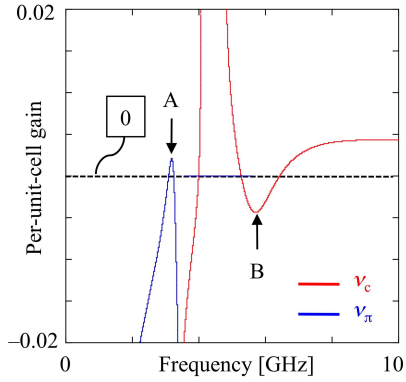

Figure 6. Per-unit-cell gains for the c- and π-modes. Red and blue curves are for the c- and π-modes, respectively. Dashed line represents the zero per-unit-cell gain, where the wave preserves its original amplitude. Regions A and B show the frequencies for wave amplification. The frequencies that yield the maximal gain are estimated to be 3.2 and 5.7 GHz for regions A and B, respectively.

following dispersion of the c- and π-modes, given by

$$k'_c(\omega) = k_c(\omega) + iG_m \frac{C_{gd}(1 - C_{Ld}L_{Rd}\omega^2)(1 - C_{Lg}L_{Rg}\omega^2)}{2C_{Ld}C_{Lg}\omega k_c(\omega)\left[k_c^2(\omega) - k_\pi^2(\omega)\right]}, \quad (10)$$

$$k'_\pi(\omega) = k_\pi(\omega) - iG_m \frac{C_{gd}(1 - C_{Ld}L_{Rd}\omega^2)(1 - C_{Lg}L_{Rg}\omega^2)}{2C_{Ld}C_{Lg}\omega k_\pi(\omega)\left[k_c^2(\omega) - k_\pi^2(\omega)\right]}. \quad (11)$$

The imaginary part of $k'_{c(\pi)}$ represents the per-unit-cell gain. In contrast to the RH waves, the amplitude of the wave increases if the imaginary part of $k'_{c(\pi)}$ becomes positive for LH waves, because the phase velocity has the opposite sign from the group velocity. By definitions, k_c is always greater than k_π; therefore, the π (c)-mode can be uniquely amplified for the LH (RH) frequencies. By adding the contribution of resistances in a similar way, we obtain Figure 6. Here, we use the reactances listed in Table 1, set all the resistances

to 0.4 Ω, and set G_m to 4.0 mS. The amplified waves are expected at the frequencies specified by A and B. The frequencies that yield the maximal gain are estimated to be 3.2 and 5.7 GHz for regions A and B, respectively. The wave numbers corresponding to the frequencies 3.2 and 5.7 GHz are respectively estimated to be 0.50 and 0.49 rad/cell; therefore, the long wavelength approximation is well satisfied for these frequencies.

3. NUMERICAL EVALUATIONS

In this section, we numerically solve the transmission equations of a 2D CRLH TWFET in the time-domain based on the fourth order Runge-Kutta method to determine the line's capability for achieving loss compensation, and to examine the validity of the design criteria discussed above. The equations to be solved are given by

$$\frac{J_{x,i,j}}{C_{Ld}} = -\frac{d}{dt}\left(W_{i,j} - W_{i-1,j} + L_{Rd}\frac{dJ_{x,i,j}}{dt} + R_d J_{x,i,j}\right), \quad (12)$$

$$\frac{J_{y,i,j}}{C_{Ld}} = -\frac{d}{dt}\left(W_{i,j} - W_{i,j-1} + L_{Rd}\frac{dJ_{y,i,j}}{dt} + R_d J_{y,i,j}\right), \quad (13)$$

$$\frac{I_{x,i,j}}{C_{Lg}} = -\frac{d}{dt}\left(V_{i,j} - V_{i-1,j} + L_{Rg}\frac{dI_{x,i,j}}{dt} + R_g I_{x,i,j}\right), \quad (14)$$

$$\frac{I_{y,i,j}}{C_{Lg}} = -\frac{d}{dt}\left(V_{i,j} - V_{i,j-1} + L_{Rg}\frac{dI_{y,i,j}}{dt} + R_g I_{y,i,j}\right), \quad (15)$$

$$\begin{aligned}\frac{W_{i,j} - V_D}{L_{Ld}} = &\left(\frac{d}{dt} + \frac{R_{ind}}{L_{Ld}}\right)\Bigg[J_{x,i,j} + J_{y,i,j} - J_{x,i+1,j} - J_{y,i,j+1} \\ &-I_{ds} - (C_{ds} + C_{gd})\frac{dW_{i,j}}{dt} + C_{gd}\frac{dV_{i,j}}{dt}\Bigg], \end{aligned} \quad (16)$$

$$\begin{aligned}\frac{V_{i,j} - V_G}{L_{Lg}} = &\left(\frac{d}{dt} + \frac{R_{ing}}{L_{Lg}}\right)\Bigg[I_{x,i,j} + I_{y,i,j} - I_{x,i+1,j} - I_{y,i,j+1} \\ &-(C_{gs} + C_{gd})\frac{dV_{i,j}}{dt} + C_{gd}\frac{dW_{i,j}}{dt}\Bigg], \end{aligned} \quad (17)$$

where $I_{x(y),i,j}$, $J_{x(y),i,j}$, $V_{i,j}$, and $W_{i,j}$ denote the gate current flowing in the x (y) direction at the (i, j)th section, drain current flowing in the x (y) direction at the (i, j)th section, gate voltage at the (i, j)th

cell, and drain voltage at the (i, j)th cell, respectively. We employ the same values of line parameters as used in the previous section.

The simple square law formula is used for I_{ds} with respect to the gate voltage V_g, i.e.,

$$I_{ds}(V_g) = \beta(V_g - V_{TO})^2, \tag{18}$$

for $V_g > V_{TO}$, and $I_{ds} = 0$ otherwise. Here, β and V_{TO} represent the transconductance coefficient and threshold voltage, respectiely. In the following, we set β and V_{TO} to $2.0\,\mathrm{mA/V^2}$ and $-1.5\,\mathrm{V}$, respectively.

The total cell number is 199×199. We first apply sinusoidal inputs at the (100, 100)-th cell to examine loss compensation for any orientation. The input frequency was set to 3.2 GHz, such that the π-mode can achieve the loss compensation uniquely. The input voltage fraction is set to $R_\pi = -0.36$. The ends of the gate and drain lines are set to the π-mode impedances ($Z_{\pi,g} = 36\,\Omega$ and $Z_{\pi,d} = 10\,\Omega$). Figures 7(a) and (b) show the steady-state voltages at $V_G = -2.0$ and $-0.5\,\mathrm{V}$, respectively. The voltage waves originate from the center cells and start to travel to the radial orientation. We can see that the waves are less attenuated in Figure 7(b) than those in Figure 7(a). In addition, the waves in Figure 7(b) are isotropic; therefore, the FET gain equally contributes to the waves in any orientation. Although some influences are observed near the corners, the π-mode impedances effectively suppress reflections.

We next consider a 2D CRLH TWFET, in which one side is interfaced with 2D RH lines that have a series inductor and shunt

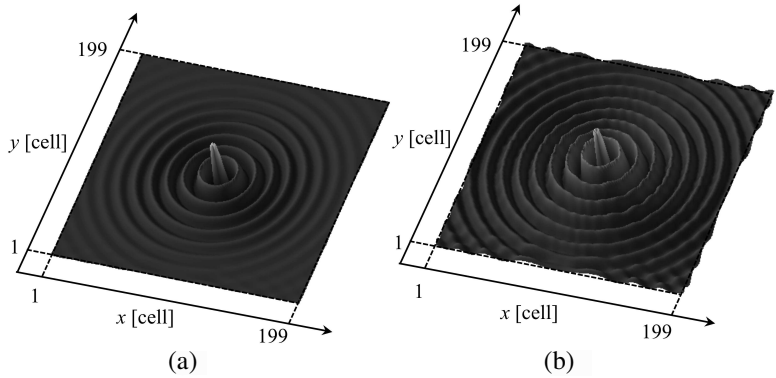

Figure 7. Calculated waveforms on 2D CRLH TWFETs. The steady-state voltage wave in the gate line is shown for (a) $V_G = -2.0\,\mathrm{V}$ and (b) $V_G = -0.5\,\mathrm{V}$.

capacitor in each of their unit cells. When the series inductance and shunt capacitance are respectively denoted as L_{RH} and C_{RH}, the characteristic impedance and wave number are given by $\sqrt{L_{RH}/C_{RH}}$ and $2\pi f\sqrt{L_{RH}C_{RH}}$, respectively, at the frequency f. For the impedance and wave number matching, we designed the impedance and wave number to be 36 Ω and 0.5 rad/cell for $f = 3.2$ GHz, respectively, for the 2D RH line interfaced with the gate line. The resulting L_{RH} and C_{RH} were set to 0.9 nH and 0.7 pF, respectively. By the similar procedure, the 2D RH line interfaced with the drain line has an inductance of 0.24 nH and a capacitance of 2.7 pF. Signals are input at the (10, 100)-th cell in the 2D CRLH TWFET with the π-mode sinusoidal waves, whose frequency and amplitude are 3.2 GHz and 200.0 mV, respectively. We set all the resistances to 0.8 Ω, and set G_m to 7.0 mS. Figure 8(a) shows the steady-state voltages. The radial waves originated from the inputs are refracted at the interface

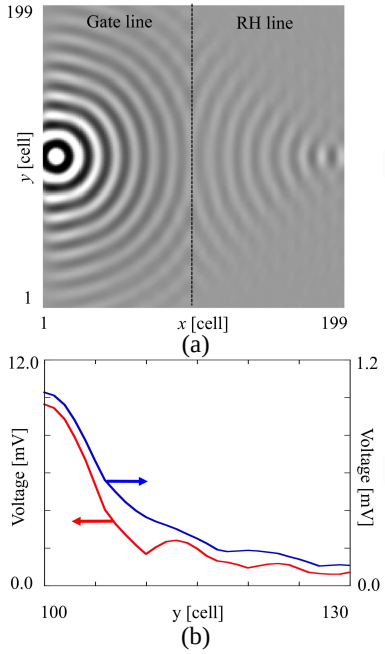

Figure 8. Wave refraction at the interface between a 2D CRLH TWFET and ordinary RH lines. (a) The steady-state voltage monitored at the gate line, and (b) tthe amplitude profile along the y axis at the image location ($x = 190$). Red and blue curves represent the profile for $V_G = -0.5$ and -2.0 V, respectively.

to be focused at the antipodal point located at the (190,100)-th cell. By impedance matching, no reflection is observed at the interface. Figure 8(b) compares the voltage profiles at $V_G = -2.0$ and $-0.5\,\mathrm{V}$. The voltage amplitude along the y orientation for $x = 190$ is plotted. The amplitude at the focus for $V_G = -0.5\,\mathrm{V}$ is ten times as large as that for $V_G = -2.0\,\mathrm{V}$. The wave components that are refracted around the edges of the interface are preserved by the FET gain for $V_G = -0.5\,\mathrm{V}$. As a result, the spot size becomes smaller for $V_G = -0.5\,\mathrm{V}$ than that for $V_G = -2.0\,\mathrm{V}$. For increasing the separation between the focus and the interface, the impact of FET gain is significant.

Recently, we found that the π-mode gains amplitudes, while the c-mode loses them through the measurements of the test 1D LH-TWFET realized on a standard breadboard. In addition, when the LH-TWFET was terminated with the π-mode characteristic impedance, the multiple reflections of waves could be effectively suppressed. Because the design criteria of 2D CRLH TWFETs are largely stemmed from those of 1D CRLH TWFET, these experimental findings are supposed to be equally established for 2D lines.

4. CONCLUSION

We characterized 2D CRLH lines coupled by transconductance for the development of non-attenuated LH and RH waves. For LH frequencies, the fast mode contributes to wave amplification, while the slow mode gains RH waves. As the field of applications widens in the future, the size of the platform where the LH waves travel is supposed to increase. A 2D CRLH TWFET has the universal function to design such a platform as required. We think that the device can apply to any existing systems using 2D LH waves and make them more practical.

ACKNOWLEDGMENT

The author would like to thank Shun Nakagawa for fruitful discussions.

REFERENCES

1. Caloz, C. and T. Itoh, *Electromagnetic Metamaterials: Transmission Line Theory and Microwave Applications*, Wiley-Interscience, New York, 2006.
2. Grbic, A. and G. V. Eleftheriades, "Overcoming the diffraction limit with a planar left-handed transmission-line lens," *Phys. Rev. Lett.*, Vol. 92, 117403-1–117403-4, Mar. 2004.

3. Lai, A., W.-Y. Wu, K. M. K. H. Leong, T. Itoh, and C. Caloz, "Quasi-optical manipulations of microwaves using metamaterial interfaces," *Proc. 2005 IEEE AP-S Int'l. Symp.*, 273–276, 2005.
4. Kaneda, T., A. Sanada, and H. Kubo, "2D beam scanning planar antenna array using composite right/left-handed leaky wave antennas," *IEICE Trans. on Electron.*, Vol. E89-C, No. 12, 1904–1911, 2006.
5. Weng, Z., Y. Jiao, G. Zhao, and F. Zhang, "Design and experiment of one dimension and two dimension metamaterial structures for directive emission," *Progress In Electromagnetics Research*, Vol. 70, 199–209, 2007.
6. Eberspacher, M. A., M. Bauer, and T. F. Eibert, "Design and analysis of an isotropic two-dimensional planar composite right/left-handed waveguide structure," *Adv. Radio Sci.*, Vol. 9, 73–78, 2011.
7. Si, L.-M., T. Jiang, K. Chang, X. Lv, L. Ran, and H. Xin, "Active microwave metamaterials incorporating ideal gain devices," *Materials*, Vol. 4, No. 1, 73–83, Jan. 2010.
8. Casares-Miranda, F. P., C. Camacho-Penalosa, and C. Caloz, "High-gain active composite right/left-handed leaky-wave antenna," *IEEE Trans. Antennas Propagat.*, Vol. 54, No. 8, 2292–2300, Aug. 2006.
9. Nakagawa, S. and K. Narahara, "Characterization of left-handed traveling-wave transistors," *IEICE Trans. Electron.*. Vol. E92-C, 1396–1400, 2009.
10. Gupta, K. C., R. Garg, and I. J. Bahl, *Microstrip Lines and Slotlines*, Artech, 1979.